



Geotechnical Testing Journal

Sara Amoroso,¹ Cesare Comina,² and Diego Marchetti³

DOI: 10.1520/GTJ20180233

Combined P- and S-Wave
Measurements by Seismic
Dilatometer Test (SPDMT):
A Case History in Bondeno
(Emilia Romagna, Italy)

Sara Amoroso,¹ Cesare Comina,² and Diego Marchetti³

Combined P- and S-Wave Measurements by Seismic Dilatometer Test (SPDMT): A Case History in Bondeno (Emilia Romagna, Italy)

Reference

S. Amoroso, C. Comina, and D. Marchetti, "Combined P- and S-Wave Measurements by Seismic Dilatometer Test (SPDMT): A Case History in Bondeno (Emilia Romagna, Italy)," *Geotechnical Testing Journal* <https://doi.org/10.1520/GTJ20180233>

ABSTRACT

A new seismic dilatometer (SPDMT) has been developed to combine the measurements of the flat dilatometer (DMT) geotechnical parameters with both P- and S- waves velocities. This new SPDMT is composed of the traditional mechanical DMT and four sensors for measuring the body waves velocities placed above the DMT blade. This SPDMT device is presented here, and the test procedure and the interpretation of P- and S-wave measurements are discussed. Results of the application of this new instrument are reported in a test site located in Bondeno (Emilia Romagna, Italy). Here, challenging water table conditions offer the opportunity to evaluate the advantage of a combined measure of the two propagation velocities, together with DMT geotechnical parameters, with the same apparatus for the porosity evaluation and a more calibrated liquefaction assessment.

Keywords

seismic dilatometer test, P-wave velocity, S-wave velocity, degree of saturation, porosity estimation, liquefaction assessment

Introduction

The development of field testing techniques has shifted the routine site investigation practices from drilling, sampling, and laboratory testing to direct in situ field testing. Today, field testing often represents the major part of geotechnical investigations with the advantage that the subsoil is tested in its natural condition with limited disturbance and that measurements may be conducted also in difficult to sample soils. This is particularly

Manuscript received July 30, 2018; accepted for publication January 28, 2019; published online April 3, 2019.

¹ Istituto Nazionale di Geofisica e Vulcanologia, L'Aquila 67100, Italy; and Department of Engineering and Geology, University of Chieti-Pescara, Viale Pindaro, 42, 65129 Pescara, Italy (Corresponding author), e-mail: sara.amoroso@ingv.it, <https://orcid.org/0000-0001-5835-079X>

² Dipartimento di Scienze della Terra, Università degli Studi di Torino, Via Valperga Caluso 35, Torino 10125, Italy, <http://orcid.org/0000-0002-3536-9890>

³ Studio Prof. Marchetti, Via Bracciano 38, Rome 00189, Italy, <http://orcid.org/0000-0002-2544-3575>

relevant for seismic wave velocity measurements for earthquake hazard purposes. Therefore, there is the need for instrumentation able to acquire multiple parameters with the same investigation tool for a more efficient approach to geotechnical site characterization, as for the addition of seismic sensors to traditional direct-push in situ tests. The most used seismic sensors are horizontal geophones or accelerometers, designed for S-wave velocity (V_S) measurements. These combined testing devices are defined as “seismic,” given the added value of the V_S measurement for the characterization (e.g., seismic dilatometer [SDMT] or seismic piezocone [SCPTU]). Recommendations in recent state-of-the-art articles (e.g., [Mayne 2016](#); [Robertson 2016](#)) indicate that direct-push in situ tests with combined V_S measurement offer clear opportunities in the economical and optimal collection of data for daily site investigations when compared with other invasive seismic tests.

Limited effort has been conversely promoted with respect to the measurement of the P-wave velocity (V_P), although V_P has been recognized as sensitive to the full-to-near-saturation transition. It can indeed happen that soil deposits below the groundwater table (*GWT*) are not, as usually assumed, fully saturated, as recently documented by [Cox et al. \(2018\)](#) and [Stokoe et al. \(2014\)](#) for more than 50 sites in Christchurch (New Zealand) using a new invasive near-surface seismic testing method, the direct-push cross-hole test (DPCH). Therefore, V_P drops from the typical value for saturated materials with low solid skeleton stiffness (i.e., above 1,450 m/s) may be indicative of partial saturation. A V_P variation from 1,450 m/s to 1,200 m/s has been measured by [Jamiolkowski, Ricceri, and Simonini \(2009\)](#), evidencing the presence of undissolved marsh gas below the Venice (Italy) sea level. The effectiveness of the use of V_P in identifying partial saturated zones has also been confirmed at a borehole array site by [Yang and Sato \(2000\)](#). The V_P capability to map the saturation surface position in the subsoil may find use in tailings deposits, characterized by a complex hydraulic regime (variable in time and space), for stability analyses, as it has been experienced for the copper tailings storage disposal at Zelazny Most (Poland) site ([Jamiolkowski 2012](#)). Moreover, V_P measurements can support the monitoring of the soil desaturation for ground improvement, as experienced by [Wotherspoon et al. \(2017\)](#) testing sandy deposits before and after the installation of stone columns in New Zealand (Christchurch).

Furthermore, laboratory tests ([Yoshimi, Tanaka, and Tokimatsu 1989](#); [Ishihara and Tsukamoto 2004](#)) have shown that the cyclic resistance ratio (*CRR*) tends to increase significantly with a decrease in V_P , particularly below 500 m/s, and when the V_P/V_S ratio drops below a value of about 3, as a consequence of the partial saturation condition. As a result, the liquefaction assessment (“simplified procedure”, [Seed and Idriss 1971](#)) can introduce a partial saturation factor (*PSF*), inferred from V_P , to correct the *CRR* and properly take into account this phenomenon ([Yang, Savidis, and Roemer 2004](#)). This allows a more reliable liquefaction assessment based on combined P- and S-wave velocity data, as recently presented by [Amoroso et al. \(2018\)](#) using DPCH and SDMT results, and by [Cox et al. \(2017\)](#) combining DPCH and piezocone (CPTU) tests in Christchurch (New Zealand). This latter case highlights the importance of the use of V_P measurements to increase the *CRR* of soils that were partially saturated below the *GWT* and to partly explain the false-positive liquefaction prediction provided using only CPTU data.

Generally, the coupled use of V_P and V_S can also support the geotechnical characterization in both static and dynamic analyses in which the elastic constants, including Poisson’s ratio (undrained estimations for saturated soils), are input variables into the models ([Finn 1984](#)). Also, according to [Foti, Lai, and Lancellotta \(2002\)](#), the theory of linear poroelastodynamics in the low-frequency limit ([Biot 1956a](#); [1956b](#)) can be used for determining the porosity in fluid-saturated porous media from V_P and V_S . This possible porosity determination has particular relevance in difficult to sample materials.

This study presents a new SPDMT recently developed to measure V_P , together with V_S and the flat dilatometer (DMT) geotechnical parameters. The new equipment is composed of the traditional mechanical DMT blade with the addition of four appropriate seismic sensors. Preliminary results on the use of this instrumentation have been already presented ([Amoroso et al. 2016](#)) showing that V_P and V_S by SPDMT are comparable with several other invasive seismic tests. Here, the SPDMT test setup and the obtained results are presented in a test site in Bondeno (Ferrara, Italy) within an ongoing detailed seismic microzonation study, following the 2012 Emilia Romagna earthquake and related liquefaction phenomena. The site has been selected because it is located in the residential area of

the municipality, and it is characterized by shallow soil deposits related to the hydrographic evolution of the Po river and its Apennine tributaries, such as the Panaro river (Stefani et al. 2018). These deposits were preliminarily identified as potentially liquefiable. The *GWT* is expected to be quite shallow because of the combined presence of the Panaro river, a stream of the Po river, that flows from the southwest to the north east through the village, and two artificial channels (Cavo Napoleonico and Canale di Burana) that border the town.

The New SPDMT

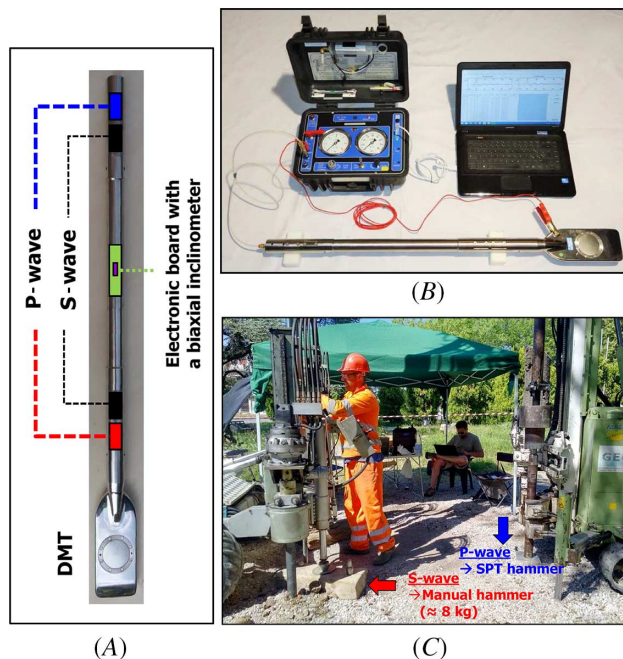
The SPDMT is the combination of the DMT equipment, standardized in ASTM D6635-15, *Standard Test Method for Performing the Flat Plate Dilatometer* (2015) with a V_p - V_s seismic probe (fig. 1). The blade provides two corrected pressure readings, p_0 and p_1 , used to determine the geotechnical parameters with the current DMT correlations (Marchetti 1980): the material index, I_D , the constrained modulus, M , the undrained shear strength, s_u , and the horizontal stress index, K_D . An additional DMT-corrected pressure reading, p_2 , may also be acquired to detect the equilibrium pore pressure, u_0 , in sandy layers, or to distinguish soil layers of different permeability.

SEISMIC INSTRUMENTATION

The seismic probe is equipped with two vertical geophones, spaced 0.6 m, for measuring V_p , along with two horizontal geophones, spaced 0.5 m, for measuring V_s (fig. 1A). Geophones have appropriate frequency and sensitivity characteristics (28 Hz and 0.600 V/ips) to determine the seismic wave train arrival according to ASTM D7400-14, *Standard Test Methods for Downhole Seismic Testing* (2014). A biaxial inclinometer is also located at the midpoint of the seismic probe (fig. 1A) to monitor the tilt during the penetration and to eventually correct V_p and V_s measurements. Two different seismic sources are used to generate P- or S-waves at the ground surface. An impulsive source hitting vertically a squared base is used for P-waves, whereas a manual or pendulum hammer hitting horizontally an appropriate base is used for S-waves (fig. 1C). The most successful solution tested

FIG. 1

Trial SPDMT- V_p : (A) DMT blade and SPDMT module; (B) SPDMT equipment; and (C) example of P-wave and S-wave seismic sources.



for generating P-wave is the combination of a heavy metal hammer, such as a standard penetration test (SPT) device, with a metal base. This metal-on-metal impact allows to generate high frequency providing higher resolution of P-wave seismograms with depth. The S-wave source, generally 10 kg heavy, is oriented parallel to the receiver axis, eventually using reverse polarity shots, to increase the sensitivity to the generated shear waves. Both P- and S-wave sources are usually located at a distance of 1 to 2 m from the penetrating rods of the DMT and connected to two different external triggers. However, when possible, it is probably best to place the shear source closer to the rods (even less than 1 m) to have the S-waves travel nearly vertical. Different consideration needs to be highlighted for the compression source, because the placement of the source at distance less than 1 m typically generates rod waves contaminating the P-wave arrivals. Special adaptors that mechanically decouple the rods from the SDMT probe have been observed, in preliminary experiments, to not be particularly useful in breaking the contact between the soil and the push rods. Further details on the seismic sources are provided for the presented case study in the next section. The seismic signal, acquired by the geophones, is amplified and digitized at depth. The recording system consists of one channel for each geophone, having identical phase characteristics and adjustable gain control. Usual sampling intervals of 50 μ s and 200 μ s are used respectively for P- and S-waves.

TESTING METHODOLOGY

Both the DMT and the seismic tests are conducted by progressively advancing the SPDMT probe and repeating the measurements at different depth intervals. The DMT measurements are usually executed at 0.2 m intervals, whereas the seismic data are acquired each 0.5 m. This depth step allows a partial superposition of the lower and the upper geophones of the seismic module in consecutive lowerings that may be potentially used for trace stacking, resulting in a single trace at the desired depth. Shot stacking at each depth, usually 3 to 5 hits, is also commonly performed both for P- and S-wave measurements.

Recorded traces are plotted as a function of depth, and the P- and S-wave arrival times (T_p) in each receiver position during penetration are determined. This determination can be based both on manual first break picking or using cross-correlation algorithms. The applicability of cross-correlation algorithms depends on the quality of the recorded traces and of the seismic pulse to be correlated. Better results are usually obtained for S-waves with respect to P-waves; for these last, manual picking can be a useful alternative. In the following, only the first break manual picking has been used for comparison. The test interpretation can rely both on the interpolation method, considering arrival times at each receiver with depth, or on the true-interval method, considering the delay between two consecutive receivers at depth.

In the first case the arrival times are corrected by the raypath inclination with:

$$T_c = \left(\frac{d}{SD} \right) \cdot T_p \quad (1)$$

where SD is the straight-line slanted travel path from the source to the receiver (assuming linear raypath), d is the depth, for each sensor, and T_p is the picked first arrival travel time, related either to P- or S-waves. All the corrected arrival times (T_c) are then plotted with depth to interpolate homogeneous velocity intervals. The interpolation method is commonly used in the analysis of downhole data (Auld 1977), and it is often convenient when layering has to be determined, reducing inaccuracies in the arrival time determination mediating among multiple data. In the true-interval method, seismic velocity is obtained as the ratio between the difference in distance among the source and the two receivers ($SD_2 - SD_1$) and their delay time ($T_{p2} - T_{p1}$).

SPDMT Survey

The area of study belongs to the external part of the Apennine chain, buried beneath the recent alluvial plain. This portion of the chain consists of blind thrust and fold structures, generated through Neogene and Quaternary times (Minarelli et al. 2016). The compressive tectonic regime is responsible for the 2012 Emilia Romagna

earthquake and for the previous historical earthquake of the area. The Bondeno test site is located in the transitional zone between the Po river alluvial plain (north sector) aggraded by sinuous meanders, detectable also by aerial photos, and the Apennine alluvial plain (south sector), formed mainly by the Panaro river (Stefani et al. 2018).

At the Bondeno site, the SPDMT sounding reached 22.6 m for the DMT readings, while V_P and V_S measurements were extended up to 30 m. The different investigation depths were related to the aim to use mainly the DMT data for the liquefaction assessment and the V_S acquisition for the ground type classification, as defined by the time-averaged shear wave velocity at the first 30 meters, $V_{S,30}$ (EN 1998-1:2004, Eurocode 8: Design of Structures for Earthquake Resistance – Part 1: General Rules, Seismic Actions and Rules for Buildings).

GEOTECHNICAL PARAMETERS

In figure 2, the obtained DMT geotechnical parameters as a function of depth are reported. According to the soil classification based on I_D , the site is characterized by silts with interbedded clays and sands in the upper 5.4 m, then clays and silty clays, with relatively low stiffness and strength parameters, are observed up to 18.8 m. Thin layers of silty sands and sandy silts are placed between 11.8 m and 13.4 m. For depths greater than 18.8 m, silty sands and sandy silts with higher stiffness are encountered. The previous lithologies may be associated with the levee of the paleochannel of the Panaro river (above 5.4 m), to the interfluvial plain deposits (5.4–18.8 m), and to the paleochannel of the Po river (below 18.8 m). Two different GWTs appear to be detected by the p_2 readings acquired in sandy layers (fig. 2). The shallow GWT can be located at a 3 m depth corresponding to the water level of the Panaro river. In contrast, the bottom GWT can be related to a confined aquifer, starting from 19 m depth, whose piezometric surface is attributed at 8 m depth. The disconnection between the two GWTs may be related to the clayey layer between a depth of 13 and 19 m.

SEISMIC VELOCITIES

In the present study, P-waves were produced using an impulsive source composed of an SPT device, with a mass of 63.5 kg and a free fall of 0.76 m, hitting vertically a 1-m-long drill rod placed on an aluminum squared base (0.2 m by 0.2 m by 0.04 m), with a mass of 3.8 kg (fig. 1C). The S-wave source was a manual hammer (10 kg) hitting horizontally a wooden rectangular base (0.5 m by 0.15 m by 0.15 m) vertically pressed against the soil (by the weight of the penetrometer, fig. 1C). The P- and S-wave sources were located at 1.6 and 1.4 m from the rods, respectively. In figure 3, the recorded traces with depth are reported with evidence of the first break picking. For both seismic waves, high-quality traces have been achieved after appropriate band pass (5–150 Hz) filtering of the raw data and stacking of the traces at superimposing geophone locations. Conversely with previous experiences,

FIG. 2 DMT parameters at the Bondeno site.

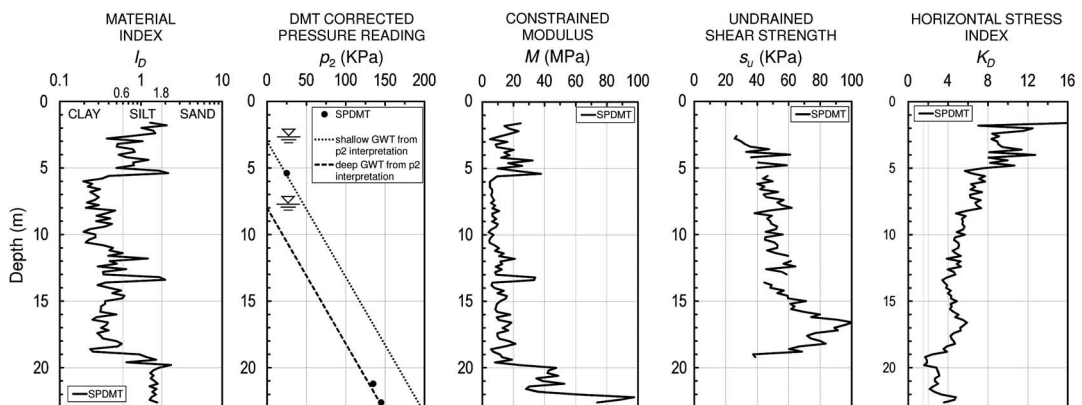
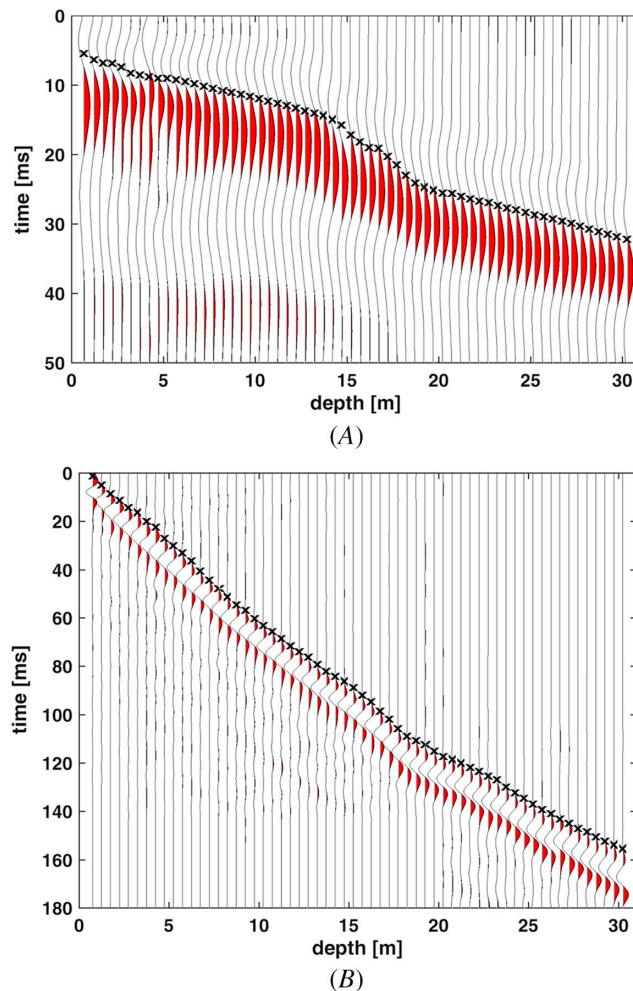


FIG. 3

SPDMT recorded seismic traces at the Bondeno site for: (A) P-waves and (B) S-waves.

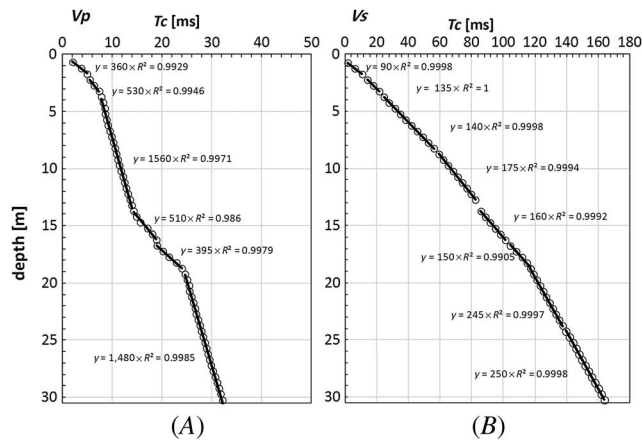


in which the P-wave measurement has been attempted (e.g., Amoroso et al. 2016), the adopted P-wave source configuration strongly reduced the rod waves influence in data acquisition. Particularly, partial rod wave influence appears only for the shallower geophone locations whereas trace quality seems to improve with depth. The oscillating nature of the seismogram prior to the first break picked is also related to the applied band pass filtering, which was necessary to remove high-frequency noise but deteriorates the trace quality. However, travel time determination for P-waves resulted more difficult. This was mainly due to the non perfect superposition of geophones locations and the oscillating nature of the arrival times in some soil layer intervals.

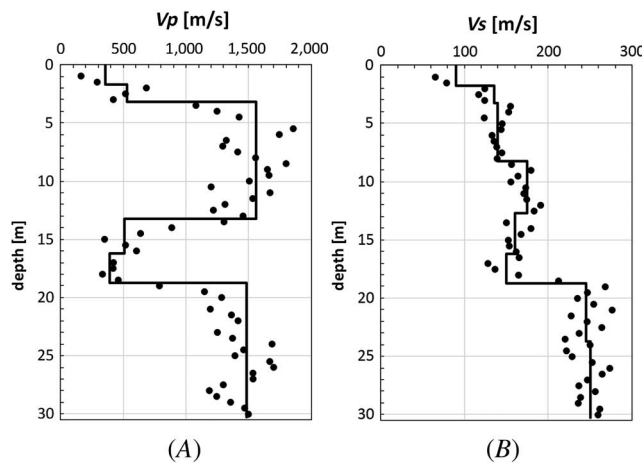
Travel time curves resulting after time correction (equation (1)) for both methods are reported in figure 4, together with the interpolating branches and resulting coefficient of determination (R^2). With the exception of only a few shallow layers having a reduced number of data points, the interpolations are performed over an average of travel time values. This layered interpretation, obtained using slope breaks evident in the corrected travel time data as shown in figure 4B, is reported in figure 5, and it is compared with the true-interval interpretation. The layered interpretation is very consistent, given the high quality of the interpolation, whereas true-interval results appears partially sparse, particularly for P-waves, because of the aforementioned difficulties in travel time determination. Nevertheless, the same velocity variability within the stratigraphy can be ascertained:

FIG. 4

SPDMT travel time curves after time correction (equation (1)): (A) P-waves and (B) S-waves.

**FIG. 5**

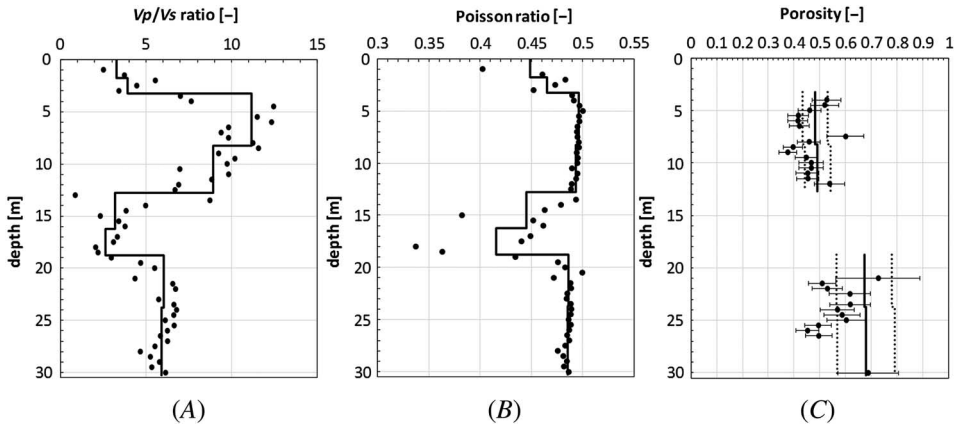
SPDMT results in terms of (A) V_P and (B) V_S at the Bondeno site; both interpolation method (continuous lines) and true-interval method (dots) are reported.



V_S data corroborate the difference between the soil deposits in the upper 19 m ($V_S \approx 150$ m/s) and the bottom paleochannel of the Po river ($V_S \approx 250$ m/s), as already found by the M profile; V_P data confirm the location of the two different aquifers preliminarily detected by DMT readings. The soil deposits appear fully saturated ($V_P \approx 1,500$ m/s) between 3 and 13 m and at depths greater than 19 m. Between these saturated layers, a V_P and small V_S velocity reduction is observed. This low V_P layer may be attributed to partially saturated clays lying above the lower sand formation hosting the confined aquifer. The presence of isolated gas bubbles may be also contemplated within this soil layer, because several gas emissions are documented in the Emilia Romagna plain (e.g., Bonzi et al. 2017).

Further interpretations of the seismic velocity data are also reported in figure 6 in terms of V_P/V_S ratio, Poisson's ratio, and porosity. This last parameter has been obtained using V_P and V_S data within the saturated layers following the formulation proposed by Foti and Passeri (2016), which provides also a closed-form formula for the propagation of parameter uncertainties. The used formulation is dependent on properties that assume rather standard values (grain density, water density, water bulk modulus) and on the Poisson's ratio of the soil skeleton. This last has a limited range of variability in soils (typically 0.1–0.2 for both clays and sands), and it can

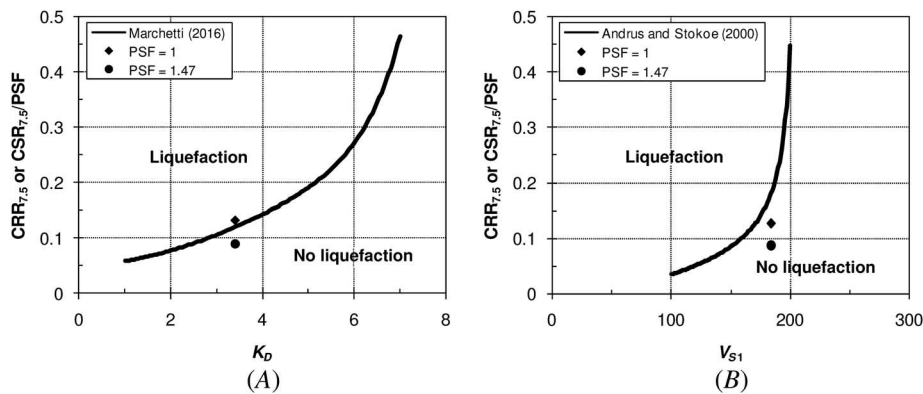
FIG. 6 SPDMT results in terms of (A) V_p/V_s ratio, (B) Poisson's ratio, and (C) porosity at the Bondeno site; both mean values within the layers (continuous lines) and local values (dots) are reported.



be shown to have negligible influence on the estimated values of porosity (Foti, Lai, and Lancellotta 2002). Coherently with the previously reported results, Poisson's ratio values (fig. 6B) are higher within the saturated layers, with typical values for saturated materials (i.e., above 0.48) with low solid skeleton stiffness. A decrease in Poisson's ratio is instead observed in the shallower layers, and between 13 and 19 m of depth, confirming a partial saturation condition of this last portion of the soil stratigraphy. This behavior is justified because Poisson's ratio values, calculated from V_p/V_s ratios, are undrained values that do not reflect the stiffness of the soil skeleton when the soil is nearly or completely saturated. The proposed Poisson's calculation is related to the small deformation level (elastic behavior) to which propagation of seismic velocities refers, and shear wave anisotropy is neglected. This last could be eventually considered, using SDMT, by adopting specific acquisition methods, which take into account of eventual transversal anisotropy (e.g., Foti et al. 2006). However, whether the soil is isotropic or not, when it is saturated, Poisson's ratio values calculated from V_p/V_s ratios will be much higher than the Poisson's ratio values for the soil skeleton, this last should be therefore assumed a priori. Both V_p/V_s ratio and porosity data (fig. 6A and 6C) report a difference in the two saturated layers, which could be related to their different constituting material. Higher V_p/V_s ratios and lower porosities are observed in the upper clayey and silty clayey layer while lower V_p/V_s ratios and relatively higher porosities are observed in the silty sands and sandy silts of the paleochannel of the Po river. However, it must be observed that the porosity values below 19 m show a higher variability and parameter uncertainty, and, also considering the DMT results, the estimated porosity could result overestimated.

The liquefaction assessment of the silty sandy layer at 13.5-m depth has been performed using the "simplified procedure." The cyclic stress ratio (CSR) at 7.5 earthquake magnitude ($CSR_{7.5}$) has been calculated (Idriss and Boulanger 2008) introducing a moment magnitude equal to 6.14 and a peak ground acceleration of 0.22 g, as provided by the seismic microzonation guidelines of Emilia Romagna Region. The CRR at 7.5 earthquake magnitude ($CRR_{7.5}$) has been estimated using both the horizontal stress index K_D (Marchetti 2016), and the overburden-stress corrected shear wave velocity V_{SI} (Andrus and Stokoe 2000). In figure 7 the results obtained introducing or not the partial saturation, by means of appropriate PSF, are reported. The partial saturation of the silty sandy layer ($PSF = 1.47$, estimated from V_p measurements) influences the soil liquefaction response, increasing the liquefaction resistance when compared with fully saturated conditions ($PSF = 1$). According to Marchetti and Monaco (2018), the $CRR_{7.5}-K_D$ prediction has to be considered more reliable with respect to the $CRR_{7.5}-V_{SI}$ one, because V_s is considerably less sensitive than K_D to stress history and because the strains at which S-waves are measured are much smaller than the strains during liquefaction. However, the non

FIG. 7 Liquefaction assessment of the silty sandy layer located at 13.50-m depth at the Bondeno site using (A) DMT data and (B) V_S measurements; the dots and the diamonds provide the results introducing the partial saturation or not, respectively.



liquefiability assessment (fig. 7A), obtained with the appropriate use of PSF and with reference to the design earthquake, appears coherent with observations of no evidence of liquefaction phenomena at this particular test site, after the 2012 earthquake, with respect to the surroundings.

Conclusions

The results presented in this article report the use of a new SPDMT to measure V_P , in addition to V_S and to DMT readings. The SPDMT outcomes have confirmed the high consistency of V_S interpretation and an acceptable confidence for V_P values even in nontrivial soil conditions.

The integration of V_P and V_S with DMT measurements strongly improved the level of knowledge of the subsoil and allowed a more comprehensive characterization of the stratigraphy. The added potentiality of measuring seismic velocities has the advantage of complementing the geotechnical characterization, particularly with respect to earthquake hazard purposes. Several Authors (e.g., Marchetti et al. 2008; Amoroso et al. 2014; Cox and Mayne 2015; Di Mariano et al. 2019) have already presented procedures to calibrate stiffness decay curves using DMT and V_S measurements. The added V_P acquisitions can further improve the geotechnical characterization facilitating the interpretation of the pore pressure and degree of saturation profiles with the combined use of p_2 data. Moreover, V_P measurements also allow for porosity evaluation within saturated layers and more calibrated liquefaction assessment within the partially saturated soil deposits.

ACKNOWLEDGMENTS

Special thanks to Luca Minarelli for sharing the information of the ongoing seismic microzonation study of Bondeno, to Maria Rosaria Manuel for supporting the proper performance of the site campaign, and to Federico Passeri for the help in interpreting the porosity data. The authors would also like to thank the anonymous reviewers for the valuable comments and suggestions to improve the article.

References

- Amoroso, S., K. M. Rollins, P. Monaco, M. Holtrigter, and A. Thorp. 2018. "Monitoring Ground Improvement Using the Seismic Dilatometer in Christchurch, New Zealand." *Geotechnical Testing Journal* 41, no. 5 (September): 946–966. <https://doi.org/10.1520/GTJ20170376>

- Amoroso, S., C. Comina, S. Foti, and D. Marchetti. 2016. "Preliminary Results of P-Wave and S-Wave Measurements by Seismic Dilatometer Test (SPDMT) in Mirandola (Italy)." In *Proceedings of 5th International Conference on Geotechnical and Geophysical Site Characterization*, 825–830. Sydney: Australian Geomechanics Society.
- Amoroso, S., P. Monaco, B. M. Lehané, and D. Marchetti. 2014. "Examination of the Potential of the Seismic Dilatometer (SDMT) to Estimate In Situ Stiffness Decay Curves in Various Soil Types." *Soils and Rocks* 37, no. 3 (September/December): 177–194.
- Andrus, R. D. and K. H. Stokoe II. 2000. "Liquefaction Resistance of Soils from Shear-Wave Velocity." *Journal of Geotechnical and Geoenvironmental Engineering* 126, no. 11 (November): 1015–1025. [https://doi.org/10.1061/\(ASCE\)1090-0241\(2000\)126:11\(1015\)](https://doi.org/10.1061/(ASCE)1090-0241(2000)126:11(1015))
- Auld, B., 1977. "Cross-Hole and Down-Hole V_s by Mechanical Impulse." *Journal of the Geotechnical Engineering Division* 103, no. 12: 1381–1398.
- ASTM International. 2014. *Standard Test Methods for Downhole Seismic Testing*. ASTM D7400–14. West Conshohocken, PA: ASTM International, approved November 1, 2014. <https://doi.org/10.1520/D7400-14>
- ASTM International. 2015. *Standard Test Method for Performing the Flat Plate Dilatometer*. ASTM D6635–15. West Conshohocken, PA: ASTM International, approved November 1, 2015. <https://doi.org/10.1520/D6635-15>
- Biot, M. A. 1956a. "Theory of Propagation of Elastic Waves in a Fluid-Saturated Porous Solid. I. Low-Frequency Range." *Journal of the Acoustical Society of America* 28, no. 2 (March): 168–178. <https://doi.org/10.1121/1.1908239>
- Biot, M. A. 1956b. "Theory of Propagation of Elastic Waves in a Fluid-Saturated Porous Solid. II. Higher Frequency Range." *Journal of the Acoustical Society of America* 28, no. 2 (March): 179–191. <https://doi.org/10.1121/1.1908241>
- Bonzi, L., V. Ferrari, G. Martinelli, E. Norelli, and P. Severi. 2017. "Unusual Geological Phenomena in the Emilia-Romagna Plain (Italy): Gas Emissions from Wells and the Ground, Hot Water Wells, Geomorphological Variations. A Review and an Update of Documented Reports." *Bollettino di Geofisica Teorica e Applicata* 58, no. 2 (June): 87–102.
- CEN European Committee for Standardization. 2004. *Eurocode 8: Design of Structures for Earthquake Resistance – Part 1: General Rules, Seismic Actions and Rules for Buildings*. EN 1998-1:2004. Brussels, Belgium: CEN European Committee for Standardization. www.cen.eu
- Cox, B. R., A. C. Stolte, K. H. Stokoe II, and L. M. Wotherspoon. 2018. "A Direct-Push Crosshole Test Method for the In-Situ Evaluation of High-Resolution P- and S-wave Velocity." *Geotechnical Testing Journal* 42, no. 5 (September). <https://doi.org/10.1520/GTJ20170382>
- Cox, B. R., K. A. McLaughlin, S. van Ballegooy, M. Cubrinovski, R. Boulanger, and L. Wotherspoon. 2017. "In-Situ Investigation of False-Positive Liquefaction Sites in Christchurch, New Zealand: St. Teresa's School Case History." In *Proceedings of Third International Conference on Performance-Based Design in Earthquake Geotechnical Engineering*. London: The International Society for Soil Mechanics and Geotechnical Engineering.
- Cox, C. and P. W. Mayne. 2015. "Soil Stiffness Constitutive Model Parameters for Geotechnical Problems: A Dilatometer Testing Approach." In *Proceedings of DMT'15 The Third International Conference on the Flat Dilatometer*, 393–400. London: The International Society for Soil Mechanics and Geotechnical Engineering.
- Di Mariano, A., S. Amoroso, M. Arroyo, P. Monaco, and A. Gens. 2019. "Case Study: SDMT-Based Numerical Analyses of a Deep Excavation in Soft Soil." *Journal of Geotechnical and Geoenvironmental Engineering* 145, no. 1 (January): 04018102. [https://doi.org/10.1061/\(ASCE\)GT.1943-5606.0001993](https://doi.org/10.1061/(ASCE)GT.1943-5606.0001993)
- Finn, W. D. L. 1984. "Dynamic Response Analysis of Soils in Engineering Practice." In *Mechanics of Engineering Materials*. New York, NY: John Wiley & Sons Ltd.
- Foti, S., C. G. Lai, and R. Lancellotta. 2002. "Porosity of Fluid-Saturated Porous Media from Measured Seismic Wave Velocities." *Géotechnique* 52, no. 5 (June): 359–373. <https://doi.org/10.1680/geot.52.5.359.38711>
- Foti, S., R. Lancellotta, D. Marchetti, P. Monaco, and G. Totani. 2006. "Interpretation of SDMT Tests in a Transversely Isotropic Medium." In *Proceedings of Second International Conference on the Flat Dilatometer*, 275–280. Lancaster, VA: In Situ Soil Testing.
- Foti, S. and F. Passeri. 2016. "Reliability of Soil Porosity Estimation from Seismic Wave Velocities." In *Proceedings of International Conference on Geotechnical and Geophysical Site Characterization*, 425–430. Sydney: Australian Geomechanics Society.
- Idriss, I. M. and R. W. Boulanger. 2008. *Soil Liquefaction during Earthquakes. ERI Report, Publ. No.MNO-12*. Oakland, CA: Earthquake Engineering Research Institute.
- Ishihara, K. and Y. Tsukamoto. 2004. "Cyclic Strength of Imperfectly Saturated Sands and Analysis of Liquefaction." *Proceedings of the Japan Academy, Series B* 80, no. 8: 372–391. <https://doi.org/10.2183/pjab.80.372>
- Jamiolkowski, M., G. Ricceri, and P. Simonini. 2009. "Safeguarding Venice from High Tides: Site Characterization and Geotechnical Problems." In *Proceedings of 17th International Conference on Soil Mechanics and Geotechnical Engineering*, 3209–3227. Amsterdam: IOS Press.
- Jamiolkowski, M. 2012. "Role of Geophysical Testing in Geotechnical Site Characterization." *Soils and Rocks* 35, no. 2 (May/August): 117–140.
- Marchetti, S. 2016. "Incorporating the Stress History Parameter K_D of DMT into the Liquefaction Correlations in Clean Uncemented Sands." *Journal of Geotechnical and Geoenvironmental Engineering* 142, no. 2 (February): 04015072. [https://doi.org/10.1061/\(ASCE\)GT.1943-5606.0001380](https://doi.org/10.1061/(ASCE)GT.1943-5606.0001380)
- Marchetti, S. 1980. "In Situ Tests by Flat Dilatometer." *Journal of the Geotechnical Engineering Division* 106, no. GT3 (March): 299–321.

- Marchetti, S. and P. Monaco. 2018. "Recent Improvements in the Use, Interpretation, and Applications of DMT and SDMT in Practice." *Geotechnical Testing Journal* 41, no. 5 (September): 837–853. <https://doi.org/10.1520/GTJ20170386>
- Marchetti, S., P. Monaco, G. Totani, and D. Marchetti. 2008. "In Situ Tests by Seismic Dilatometer (SDMT)." In *From Research to Practice in Geotechnical Engineering*, ASCE, *Geotechnical Special Publication*, edited by J. E. Laier, D. K. Crapps, M. H. Hussein, 180: 292–311.
- Mayne, P. W. 2016. "Evaluating Effective Stress Parameters and Undrained Shear Strengths of Soft-Firm Clays from CPTU and DMT." *Australian Geomechanics Journal* 51, no. 4 (December): 27–55.
- Minarelli, L., S. Amoroso, G. Tarabusi, M. Stefani, and G. Pulelli. 2016. "Down-Hole Geophysical Characterization of Middle-Upper Quaternary Sequences in the Apennine Foredeep, Mirabello, Italy." *Annales Geophysicae* 59, no. 5 (October): S0543.
- Robertson, P. K. 2016. "Cone Penetration (CPT)-Based Soil Behavior Type (SBT) Classification System— An Update." *Canadian Geotechnical Journal* 53, no. 12 (December): 1910–1927. <https://doi.org/10.1139/cgj-2016-0044>
- Seed, H. B. and I. M. Idriss. 1971. "Simplified Procedure for Evaluating Soil Liquefaction Potential." *Journal of the Geotechnical Engineering Division* 97, no. 9 (September): 1249–1273.
- Stefani, S., L. Minarelli, A. Fontana, and I. Hajdas. 2018. "Regional Deformation of Late Quaternary Fluvial Sediments in the Apennines Foreland Basin (Emilia, Italy)." *International Journal of Earth Sciences* 107, no. 7 (October): 2433–2447. <https://doi.org/10.1007/s00531-018-1606-x>
- Stokoe, K. H., II, J. N. Roberts, S. Hwang, B. Cox, F. Y. Menq, and S. van Ballegooy. 2014. "Effectiveness of Inhibiting Liquefaction Triggering by Shallow Ground Improvement Methods: Initial Field Shaking Trials with T-Rex at One Site in Christchurch, New Zealand." In *Soil Liquefaction during Recent Large-Scale Earthquakes*, 193–202. Boca Raton, FL: CRC Press.
- Wotherspoon, L. M., B. R. Cox, K. H. Stokoe, D. J. Ashfield, and R. Phillips. 2017. "Assessment of the Degree of Soil Stiffening from Stone Column Installation Using Direct Push Crosshole Testing." In *Proceedings of the 16th World Conference on Earthquake Engineering*. Oakland, CA: Earthquake Engineering Research Institute.
- Yang, J. and T. Sato. 2000. "Interpretation of Seismic Vertical Amplification at an Array Site." *Bulletin of the Seismological Society of America* 90, no. 2 (April): 275–285. <https://doi.org/10.1785/0119990068>
- Yang, J., S. Savidis, and M. Roemer. 2004. "Evaluating Liquefaction Strength of Partially Saturated Sand." *Journal of Geotechnical and Geoenvironmental Engineering* 130, no. 9 (September): 975–979. [https://doi.org/10.1061/\(ASCE\)1090-0241\(2004\)130:9\(975\)](https://doi.org/10.1061/(ASCE)1090-0241(2004)130:9(975))
- Yoshimi, Y., K. Tanaka, and K. Tokimatsu. 1989. "Liquefaction Resistance of a Partially Saturated Sand." *Soils and Foundations* 29, no. 3 (March): 157–162. https://doi.org/10.3208/sandf1972.29.3_157